Dimensional Variation Tolerant Inverse Designed Broadband Mode Converter

Md Mahadi Masnad[1], Guowu Zhang[1], Dan-Xia Xu[2], Yuri Grinberg[3], Odile Liboiron-Ladouceur[1]
[1]Electrical and Computer Engineering Department, McGill University, Montréal, Canada
[2] Advanced Electronics and Photonics Research Center, [3] Digital Technologies Research Center, National Research Council, Ottawa, Canada
md.masnad@mail.mcgill.ca

Abstract: We report on a low-loss (<1dB) TE1-TE3 mode converter, robust to ±10 nm etch-errors, operating over a wavelength range of 1.5-1.58 µm with modal crosstalk below -20dB. 20 GBaud PAM-4 signal transmission validates the conversion.

1. Introduction

In the optical communication system, the demand for higher data transmission capacity requires deployment of various multiplexing techniques, such as wavelength-division multiplexing (WDM), time-division multiplexing (TDM), polarization-division multiplexing (PDM), and mode-division multiplexing (MDM), a relatively new method. MDM scales up the data transmission capacity by many folds without incurring additional energy budget [1]. Since only the fundamental mode is coupled to the grating coupler, the most common fiber to chip interfacing component, most efficiently, mode converters have important applications in on-chip mode conversion for mode-division multiplexed data-signals [2]. Dense integration of such photonic components demands for small-footprint design blocks. Various inverse design techniques have received much attention recently to design compact photonic devices without compromising the performance [3,4], compared to large-footprint devices designed in traditional approaches [5].

In this work, we demonstrate a quasi-TE1 to quasi-TE3 mode converter with a footprint of only 4×2 µm^2, designed using the shape optimization method, a computationally efficient inverse design method [6]. Simulation results show the mode conversion efficiency is above 95% across a 100 nm wavelength span (1.5 – 1.6 µm), and with ±10 nm etch errors, the conversion efficiencies remain above 91.7%. Continuous wave (CW) measurement of the transmission spectra shows good agreement with the simulation results, with insertion loss ranging from 0.1 dB to 1 dB across the bandwidth. The modal crosstalk is below -20 dB in the C-band. We also performed 28 Gbps on-off keying (OOK) and 20 GBaud 4-level pulse amplitude modulation (PAM-4) data transmission measurements. Despite the enormous coupling loss of the grating coupler, the minimum insertion loss of 20 dB back-to-back at 1.54 µm, we observe open eye diagrams with a Q-factor of 7.97 dB after passing through the EDFA. For ease of discussion, we often drop the “quasi” term and simply refer to the modes as TE modes.

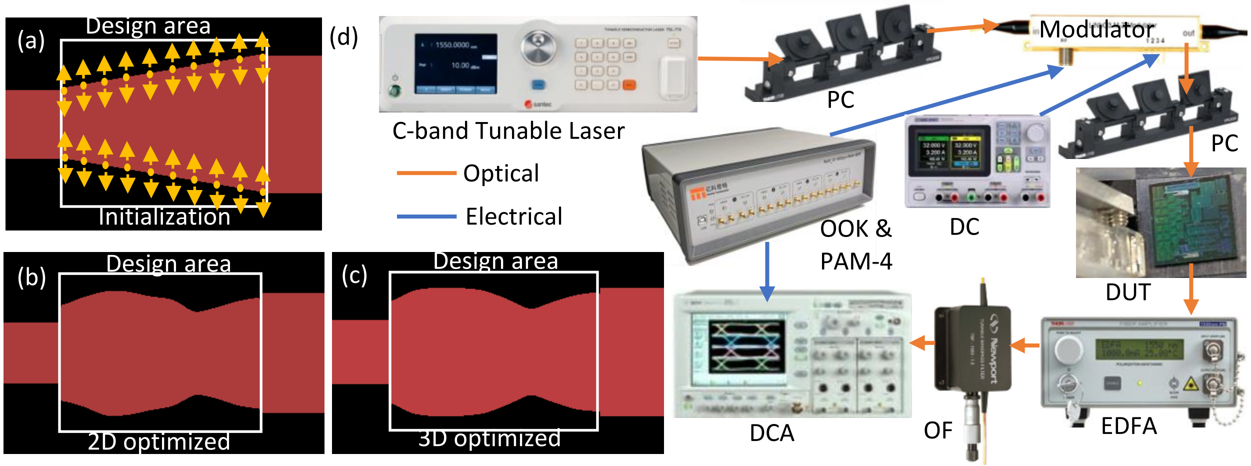

Fig. 1 Design steps: (a) Initialization with a random structure, (b) 2D optimized quasi TE1- quasi TE3 mode converter with FOM = 0.9437, (c) 3D optimized mode converter with FOM = 0.977. (d) Experimental setup for 28 Gbps on-off keying (OOK) and 20 Gbd 4-level pulse amplitude modulation (PAM-4) measurement. PC: polarization controller, DC: bias voltage supply, DUT: device under test, EDFA: erbium-doped fiber amplifier, OF: optical filter, DCA: digital communication analyzer.

2. Design Approach and Experimental Setup

In the shape optimization method, the designer first chooses the positions of and the spacing between the input and the output (I/O) waveguides, while their dimensions are usually determined by the application and the interfacing with the rest of the circuit. The optimization can begin with any random structure in the design area connecting the I/O waveguides. As shown in the Fig. 1(a), several boundary points on the structure are taken as the design parameters. With a forward and an adjoint simulations, the optimization algorithm calculates the gradient with respect to all the design parameters in a single iteration and moves around the parameter points to come up with a shape which maximizes a figure of merit (FOM). Here the FOM is defined as the optical field overlap with the designer specified mode in the output wave guide. We used the limited-memory Broyden-Fletcher-Goldfarb-Shanno bound-constrained (L_BFGS-B) algorithm to optimize the design [7]. The dimensions and the positions of the I/O waveguides and their spacing (the design footprint) determine the design parameter space, while the initial structure leads the algorithm to the nearest optimum. The mode converter is first optimized using 2D simulations in the Lumerical MODE solver which is fast; it completes around 46 iterations in an hour in a single-core personal computer. If the FOM in 2D optimization exceeds 90%, the 2D optimized parameters are used as the starting point for the final optimization using 3D FDTD simulations. 200 points on each side-boundary were interpolated from the parameter points to define a smooth geometry. Fig. 1(b) and (c) show the 2D and 3D optimized mode converters, respectively. The spacing between the I/O waveguides was varied from 3.2 μm to 4.2 μm. The final design is 4 μm long, beyond which the device performance does not improve significantly. The mode converter is designed for fabrication at Applied Nano Tools Inc (ANT) on a silicon-on-insulator (SOI) wafer with a 220 nm thick Si layer on 2 μm thick buried oxide. Fig. 1(d) shows the experimental setup for on-off keying on-off keying (OOK) and 4-level pulse amplitude modulation (PAM-4) signal transmission through the mode converter.

3. Performance Analysis

Fig. 2 (a) shows the dimensions of the quasi TE1- quasi TE3 mode converter. Since the PDK grating coupler is designed for coupling the fundamental mode only, we used tapered directional coupler-based mode (de)multiplexer to excite and separate different quasi-TE modes [8]. The electric field y-component distribution is shown in Fig. 2(b), which shows how the mode conversion happens in the design area. While TE1 mode has two lobes, TE3 mode has four; both mode profiles are antisymmetric along the y-axis. Therefore, the conversion the TE1 mode into TE3 mode requires a π-phase shift on half of the wavefront on each of the lobes of TE1 mode, while the field amplitude distribution rearranges itself to match the TE3 mode profile in the wider waveguide, as different parts of the wavefront travel different optical paths inside the design area [9]. The mode converter is bidirectional; input TE1 mode through the narrower waveguide is converted to TE3 mode in the wider waveguide and vice versa. Fig. 2 (c) shows the transmission into desired TE3 mode when the input signal is TE1 mode in the narrower waveguide and the transmissions into other undesired modes, i.e., modal crosstalk. We find TE1-TE1 to be the dominant crosstalk, while transmissions into TE0 and TE2 are below -22 dB across the wavelength range of 1.5 μm to 1.58 μm. The mode converter was optimized to operate across a 100 nm bandwidth between 1.5-1.6 μm. However, the grating coupler causes unwanted fluctuations in the transmission spectrum at the longer wavelengths. The fluctuations

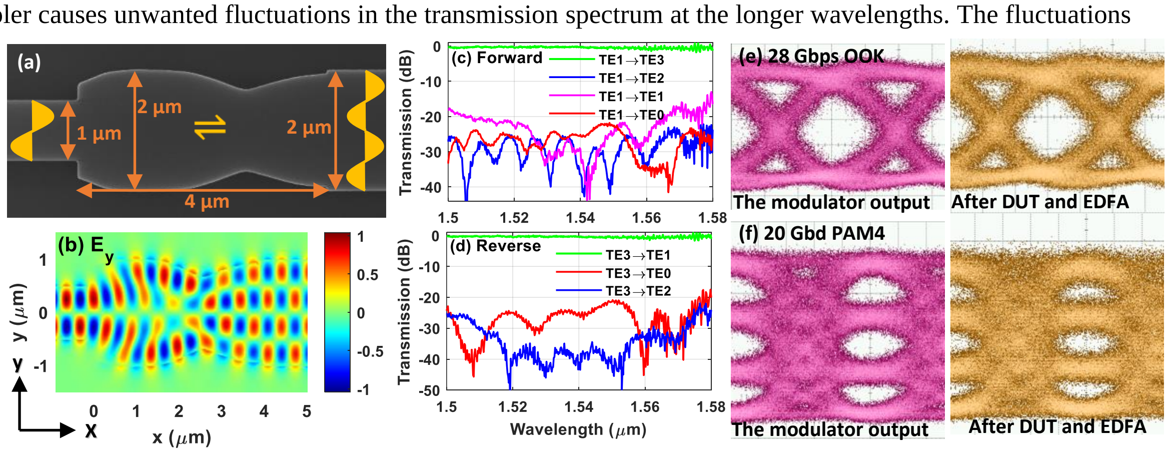

Fig. 2 (a) SEM image of the mode converter and its footprint, (b) Electric field y-component distribution, (c) Transmission from TE1 mode to TE3 mode and modal crosstalk, (d) Transmission from TE3 mode to TE1 mode and modal crosstalk, (e) Eye diagrams for 28 Gbps OOK, Q-factor = 8.41 dB at the modulator output (magenta) and Q-factor = 7.97 dB after going through the chip and EDFA (yellow), (f) Eye diagram for 20 GBd PAM-4 signal transmission at the modulator output (magenta) and the EDFA output (yellow).

beyond 1.58 μm wavelength is so high that the transmission data beyond 1.58 μm is not reported. Fig. 2(d) shows the transmission into TE1 mode and corresponding crosstalk in the narrower waveguide, when the input mode was TE3 in the wider waveguide. The insertion loss ranges from 0.1 dB to 1 dB across the wavelength range of 1.5 – 1.58 μm. Fig. 2(e) shows the eye diagrams for modulator output and after it goes through the chip and EDFA at the data rate of 28 Gbps. The Q-factor degrades from 8.41 dB to 7.97 dB, mainly due to the noise contributed by the EDFA as the mode converter is a passive device unlikely to contribute any noise. Similarly, the eye diagrams for PAM-4 signal are shown in Fig. 2(f) for 20 GBaud.

We also investigate the effects of dimensional variations such as under and over etch on the device performance by intentionally expanding and shrinking the design boundary on both sides by 10 nm to mimic the effect of under and over etches, respectively, as shown in the Fig. 3(a). For under etch, the transmission peak, combined crosstalk minima, and the peak mode conversion efficiency shift toward longer wavelengths. On the other hand, for over etch, they shift in toward the shorter wavelengths. From the graphs shown in Fig. 3(b) and (c), despite having 10 nm under/over etch the mode converter has good extinction ratio across the entire bandwidth, and the transmission into the desired mode drops only by ~0.4 dB at 1.54 μm. The final optimized mode converter has abrupt width variations with the I/O waveguides. We also optimized additional mode converter designs which makes smoother connections with the waveguides with the corner points (red) held fixed in their initial positions as shown in Fig. 3(d). Implementing this constraint consistently resulted in lower mode conversion efficiency as indicated by the dashed-black curve in Fig. 3(e).

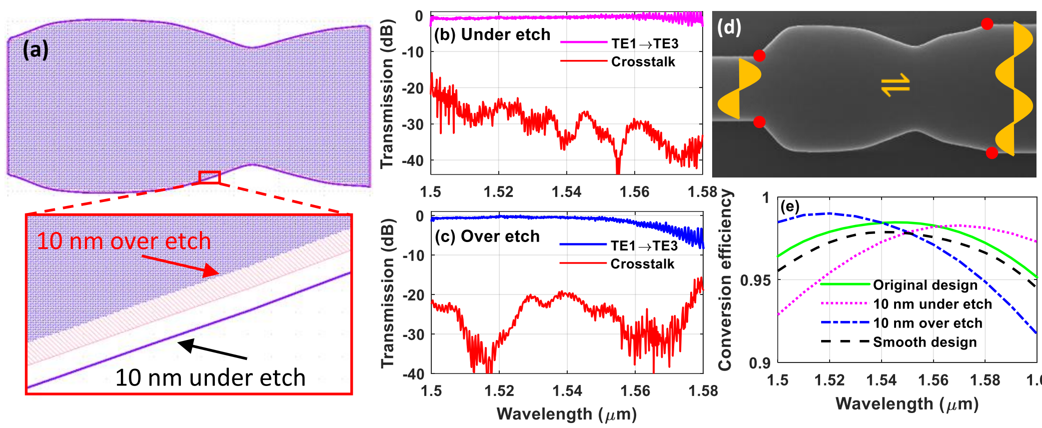

Fig. 3 (a) Illustration of 10 nm under and over etch, Transmission from TE1 mode to TE3 mode and the combined crosstalk in (b) the under etched mode converter and (c) the over etched mode converter, (d) SEM image of the smooth geometry mode converter, (e) simulation results of the mode conversion efficiencies for different variations of the original design.

4. Conclusion

We have demonstrated compact footprint TE1-TE3 mode converter designed using the shape optimization method. With a small number of design parameters, shape optimization method is computationally efficient since it converges to the final design in lower number of iterations, compared to other inverse design methods such as topology optimization. The mode converter has conversion efficiency above 95% over a wavelength range of 1.5-1.6 μm and the maximum insertion loss of 1 dB. The modal crosstalk is below -20 dB in the C-band. Despite introducing ±10 nm dimensional variations to mimic the under and over etch errors, it maintains good extinction ratio throughout the 80 nm wavelength span. Additionally, we have shown open eye diagrams for 28 Gbps OOK and 20 Gbd PAM-4 signal transmissions, despite 20 dB back-to-back coupling loss of the grating coupler at 1.54 μm.

5. References

[1] L. W. Luo *et al.*, "WDM-compatible mode-division multiplexing on a silicon chip," *Nature Commun.*, vol. 5, no. 1, pp. 1–7 (2014).
[2] V. Liu, D. A. B. Miller, and S. Fan, "Ultra-compact photonic crystal waveguide ...", *Optics express*, vol. 20, no. 27, pp. 28388-28397 (2012).
[3] J. Lu and J. Vučković, "Objective-first design of high-efficiency, small-footprint …," *Optics Express*, vol. 20, no. 7, pp. 7221-7236 (2012).
[4] A. Y. Piggott *et. al.*, "Inverse-designed photonics for semiconductor foundries," *ACS Photonics* vol. 7, no. 3, pp. 569-575 (2020).
[5] R. B. Priti, and O. Liboiron-Ladouceur, "Reconfigurable and scalable …," *Journal of Lightwave Technology* **37** (15), pp. 3851-3860 (2019).
[6] M. M. Masnad, D. Xu, Y. Grinberg, and O. Liboiron-Ladouceur, "Computationally efficient and …," *IEEE Photonics Conference* (2021).
[7] C. Zhu, R. H. Byrd, P. Lu, and J. Nocedal, "Algorithm …," *ACM Transactions on Mathematical Software*, vol. 23, no. 4, pp. 550-560 (1997).
[8] A. Das, G. Zhang, H. R. Mojaver, and O. Liboiron-Ladouceur, *IEEE Photonics Technology Letters*, vol. 33, no. 11, pp. 557-560 (2021).
[9] M. M. Masnad, Y. Grinberg, D. Xu, and O. Liboiron-Ladouceur, "Physics-guided …," OSA Photonics in Switching and Computing (2021).